

## Scalable and low-cost MEMS-based Structural Health Monitoring System

Izquierdo, Alberto<sup>1</sup>; Villacorta, Juan J.<sup>1</sup>; del Val, Lara<sup>2</sup>; and Magdaleno, Álvaro<sup>2</sup>

### ABSTRACT

This paper presents a scalable low-cost Structural Health Monitoring (SHM) system based on multiple myRIO platforms and digital MEMS (Micro Electro-Mechanical Systems) triaxial accelerometers. The system acquires the accelerations and also computes the corresponding frequency response functions for the subsequent modal analysis. This proposed SHM system was first validated using only a single board with some accelerometers on a timber beam. And after that, a larger system composed by several slave boards connected and synchronized to a master one was deployed on a timber platform to estimate its modal properties. In both scenarios, the obtained results were compared with measured by a conventional SHM system based on piezoelectric accelerometers. After carrying out these validation tests, a high correlation can be appreciated in the behaviour of both systems, concluding that the proposed system is sufficiently accurate and sensitive for operative purposes, and significantly more affordable than a traditional one.

*Keywords: Scalable, low-cost, SHM, MEMS accelerometers, Experimental Modal Analysis*

### 1. INTRODUCTION

During the last decades, the concern about the preservation of structures and infrastructures has been constantly increasing, but the high number of historical buildings and civil structures that need to be monitored makes it a complicated and barely affordable problem. The need for cost-effective systems capable of detecting and recording the dynamical response of large and relevant structures is undeniable. Non-destructive techniques (NDT) and those which are little or non-invasive for the structure under study are the most interesting procedures to assess the state of potentially damaged buildings. The application of such techniques helps the companies and governments to foresee maintenance works, which imply important economical savings and environmental care.

Among these techniques, those based on monitoring the dynamical response of the structure have attracted much interest during the last few years [1], as they are robust and harmless for the structure under test. With a set of well-placed sensors, a series of time signals can be collected from the structure and processed to estimate its modal or physical properties. The evolution of these properties over time can be helpful to assess the actual state of a structure and locate the potential damage it may suffer [2,3]. For these techniques, the sensors need to be permanently installed on the structure to be truly effective, continuously recording the structural response, transferring the recorded data to a remote

---

<sup>1</sup> *Signal Theory and Communications and Telematics Engineering Department. University of Valladolid (SPAIN). E-mail addresses: alberto.izquierdo@uva.es (Corresponding author), juavil@tel.uva.es*

<sup>2</sup> *Industrial Engineering School. University of Valladolid (SPAIN). E-mail addresses: lvalpue@eii.uva.es, alvaro.magdaleno@uva.es*

server and providing trustfully information about its current state [1,4–6]. But nowadays, this is a hard challenge that commercial structural health monitoring (SHM) systems are not fully prepared to undertake, as only few of them are conceived to work continuously. Additionally, commercially available SHM systems has another important restraint: its cost.

Due to their versatility, durability and reduced cost, accelerometers are mainly used to perform continuous monitoring of the dynamical structural response [7]. This type of sensor is intended to measure the acceleration response of a certain point of the structure in one, two or three directions, in order to estimate the modal properties of the structure: natural frequencies, damping ratios and mode shapes [8]. There exist a variety of types of accelerometers used in SHM systems, being the ones based on piezoelectric crystals and those embedded in Micro Electro-Mechanical Systems (MEMS) the most spread ones [9-11]. Piezoelectric sensors produce higher quality measurements than MEMS sensors, but at a significant higher cost.

SHM systems must comprise not only sensors but also a suitable data logger for acquiring data from them and processing the registered signals. Such integrated systems remain a challenge, and there are very few commercially available systems at a great cost [12,13]. To overcome this, the use of digital platforms integrating microprocessors and field-programmable gate arrays (FPGA) are proposed. Synchronous acquisition is attended by the FPGA while the processor operates with the previously registered signals.

This work shows a low-cost SHM system based on the use of wireless networks to monitor buildings, together with the use of MEMS accelerometers. A scalable, modular and reconfigurable system architecture, which includes modules of acquisition, processing and analysis for a SHM system, has been developed. This system can record multiple channels at high acquisition rates, like some other expensive commercial datalogger systems, and then, sequentially, process and evaluate the recorded information. It must be remarked that these abilities are not included jointly in standard commercial systems. In order to validate the developed system, one test with one monitoring device was carried out on a timber structure and, in order to verify the synchronization procedure of the system, a second test with three synchronized devices deployed on a medium-sized structure were performed. In both tests, both structures were simultaneously instrumented by using the proposed system and a standard commercial reference system, based on piezoelectric accelerometers and the SIRIUS® datalogger from Dewesoft®[14], specifically designed for this type of analysis.

The manuscript is organized as follows. Section 2 is devoted to show the low-cost device. Section 3 presents the structures, the sensor set-ups, the recording configuration and the subsequent analysis details used in the validation tests, as well as the main results that were obtained. Finally, Section 5 presents the main conclusions and remarks.

## **2. SYSTEM DESCRIPTION**

The main objective of the designed low-cost system is to allow the monitoring of different structures using digital MEMS accelerometers. Taking this objective into account, the system must be scalable, allowing the number of used accelerometers to be varied, and reconfigurable, so that the location of the sensors could be changed to adapt the set-up to the structure to be measured. Besides, the system must also be distributed, consisting of a set of autonomous modules connected wirelessly. Each of the

modules must be able to acquire and process data from a set of sensors by exchanging synchronization information with the other modules and with the control module. The final structural properties, computed from the registered signals, will help to decide about the structural integrity.

Thinking about the system requirements, it will be useful that the system should be able to:

- Generate proper input signals to command the excitation devices (for example, an inertial shaker with different patterns: noise, tones, frequency sweeps, etc.)
- Acquire and integrate information from other sensors (load cells, temperature, humidity, etc.), both analogue and digital.
- Have the possibility of autonomous operation with recording in a cloud database.

## 2.1. System Architecture

The system architecture that has been defined selected is shown in Fig. 1. The system is formed by the sensors, the adaptation units, called the Back-end units (BE-U), the Processing unit (P-U) and the control unit, called the Front-end unit (FE-U).

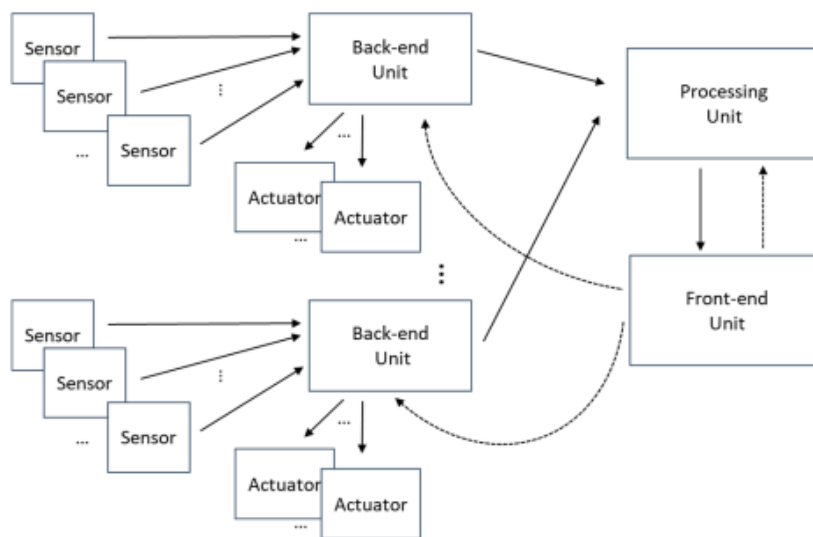


Figure 1. System architecture.

The system's sensors, mainly accelerometers, are divided into groups and managed by a set of BE-Us, which configure and read the data provided by each sensor. The system's actuators, such as shakers or pneumatic hammers, are also associated to a back-end unit, which will generate and transfer the actuation signals to the device. The sensor data obtained by the BE-Us are transferred to the P-U, that pre-processes the signals in the time domain (filtering, decimation, etc.) and calculates the FRFs and stores the processing results in a cloud-based database. Finally, the FE-U oversees the measurement and calculation process, establishes the intervals in which the measurements are made and configures the rest of the elements of the system. The FE-U also interacts with the user, allowing the visualization of the measurements and the obtained results.

## 2.2. Sensor Description

The selected accelerometer was the ADXL355 digital MEMS accelerometer, developed by Analog Devices [15], which is shown in Fig. 2a. These accelerometers measure vibrations with high resolution and very low noise to allow the early detection of structural failures, using wireless sensor networks. Their low power consumption allows for extended product use by prolonging the time between battery changes.



Figure 2. (a) ADXL355 accelerometer (b) adaptor board (c) 3D printed box (d) sensor assembled.

The ADXL355 is a low power 3-axis accelerometer with selectable measurement ranges between  $\pm 2$  g,  $\pm 4$  g, and  $\pm 8$  g. It integrates a 20 bits sigma-delta ADC (Analog to Digital Converter) per axis, corresponding with  $3.9 \mu\text{g}/\text{LSB}$  (least significant bit),  $7.8 \mu\text{g}/\text{LSB}$  and  $15.6 \mu\text{g}/\text{LSB}$  mV/g sensitivities, with respect to the defined measurement ranges. It also has a noise density of  $25 \mu\text{g}/\sqrt{\text{Hz}}$ , and a bandwidth up to 1500 Hz.

A small adaptor board has been developed to join the sensor to a RJ45 connector, as can be observed in Figure 2b. The whole set has been encapsulated in a little box that has been 3D printed (Figure 2c). This box provides mechanical integrity to the sensor and provides an anchoring mechanism to the structure to be measured. Figure 2d shows the final sensor encapsulated in the box.

## 2.3. Back-End Unit (BE-U)

Due to its flexibility in the control of the inputs and outputs and its high capacity to parallelize, a FPGA is the most suitable hardware to implement the BE-U. To avoid the complexity and high development time related with this approach, a myRIO platform [16] has been selected as the base for the BE-U. This platform is oriented to sensors with nonstandard acquisition procedures, allowing low-level programming of the acquisition routines using the LabVIEW graphical programming language. Specifically, the myRIO platform is an embedded hardware based on a Xilinx Zynq 7010 chip, which incorporates a FPGA, a dual-core ARM<sup>®</sup> (Advanced RISC Machine) Cortex<sup>™</sup>-A9 processor and two MXP ports, all this enclosed in a small box (136 mm x 89 mm x 25 mm).

Both MXP ports with 16 digital input/output (I/O) lines of the FPGA have been used to connect the myRIO platform to the ADXL355 sensors, using a self-developed MXP-to-RJ45 adaptor board with 3 RJ45 connectors, as can be observed in Fig. 3. As each of these sensors needs 5 I/O lines, up to 6 sensors can be attached to a myRIO without multiplexing I/O lines. As far as the FPGA has 40 digital I/O lines, up to 16 sensors could be connected to a single myRIO if needed.



**Figure 3.** MyRIO device with two adapter boards and an accelerometer.

The FPGA also has 2 AD inputs, which have been used to acquire analog data from other devices (like analog accelerometers or a load cell), synchronously with the digital data from the ADXL355 sensors, and 2 DA outputs, which have been employed to generate excitation signals to be used as the source to shakers or other type of modal exciters. And the ARM processor is equipped with 256 MB of DDR3 RAM (Double Data Rate 3 Random-Access Memory), 512 MB of built-in storage space, USB Host port, and Wi-Fi interface.

If several myRIO platforms are included in the system, a synchronization mechanism will be used to ensure that the data from all the accelerometers is acquired simultaneously. In this situation, one of the myRIO devices, as the master, will generate a synchronize signal, which will be used by the rest of the myRIOs (slaves) to start the acquisition synchronously.

#### **2.4. Processing and Front-End Units (P-U and FE-U)**

On the one hand, a PC is usually used to implement both the P-U and the FE-U, while one or several myRIO devices work as BE-U. In this configuration, the PC would perform two main functions:

- As a FE-U, the PC manages all the myRIO platforms connected to the system, using a Wi-Fi interface. The PC sends the configuration of the accelerometer sensors attached to each myRIO device, controls when the acquisition starts and when it stops, and receives the acquired data from the accelerometers for further processing. In addition, the PC shows a user interface that allows changing the system parameters and visualizing the results of the modal analysis of the structure.
- As a P-U, the PC could execute additional algorithms to perform the modal analysis, evaluate structural changes or generate early warning signals, among others.

On the other hand, the ARM processor of the myRIO platform could also be used to implement the PU, the FE-U, and also the BE-U, simultaneously, defining a stand-alone system.

### 3. SYSTEM VALIDATION

As it was mention in the Introduction, the proposed system has been validated with two tests, comparing its performance with a standard commercial reference system and high-end piezo-electric accelerometers, placed side-by-side with the digital MEMS accelerometers on the test structures. The Dewesoft platform has been selected as this reference system in both validation tests. Dewesoft platform is composed of:

- A DS-SIRIUS DAQ [14] device, specifically a DS-SIRIUS-8xACC-8xAO with 8 input and 8 output channels. DS-SIRIUS is a dual-core 24-bit data logger with an anti-aliasing filter on each channel with up to 200 kS/s sampling rate and 160 dB of dynamic range in the time and frequency domains. It is intended for IEPE (Integrated Electronics Piezo-Electric) sensors and supplies a configurable voltage (up to 10 V) and current (between 4 and 8 mA). The power consumption per channel is 1W.
- Six KS76C.100 [17] accelerometers, which are intended for standard applications in laboratory and industry, for vibrations between 0.5 and 70 kHz, and require a current supply ranging between 2 and 20 mA. Its acceleration range is  $\pm 60$  g with a sensitivity of  $100 \pm 5$  mV/g and 3  $\mu\text{g}/\text{VHz}$  noise density value.
- DewesoftX data acquisition software.

Table 1 shows the most relevant characteristics of the reference and the proposed systems.

**Table 1.** Main characteristics of the proposed and reference system

Characteristic	Reference System	Proposed System
Range	$\pm 60$ g	$\pm 2$ g, $\pm 4$ g and $\pm 8$ g
Digital sensitivity	11.9 $\mu\text{g}/\text{LSB}$	3.9, 7.8 and 15.6 $\mu\text{g}/\text{LSB}$
Noise density	3 $\mu\text{g}/\text{VHz}$	25 $\mu\text{g}/\text{VHz}$
Maximum sample frequency	200 kHz	4 kHz
Bits per simple	24	20
Maximum accelerometer channels	8 uni-axial	6 tri-axial
Cost (1 device + 6 accel. system configuration)	9050 €	928 €
(3-devices + 12 accel. system configuration)	11600 €	2436 €

#### 3.1. Validation tests layouts

##### 3.1.1. One-device system configuration

To carry out these first tests, a sawn timber beam of Scots pine (*Pinus sylvestris* L.) with a nominal section of 90 mm x 140 mm and a length of 5000 mm was used. This timber beam was placed on a wooden support, placed also on a steel frame. It lies in a horizontal position (140 mm) with a separation between supports of 4500 mm, as can be observed on Fig. 4. It is instrumented with 5 pairs of accelerometers (each one with a KS76C.100 and a ADXL355) evenly distributed on the timber beam (750 mm of separation), at the positions marked as E1 to E5 on Fig. 4. The beam is excited with an electromechanical shaker placed at 1500 mm from the right support, and with another pair of accelerometers placed on its moving mass (labelled as D in Fig. 4) to record the input force. In the test

layout shown in Fig. 4, the timber beam is marked with an A, the myRIO device with a B, and the shaker with a C.

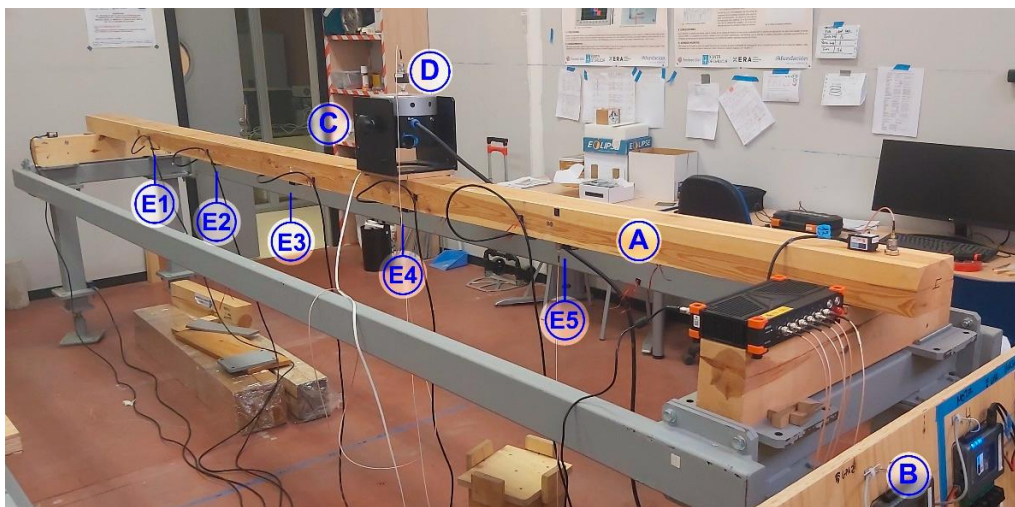
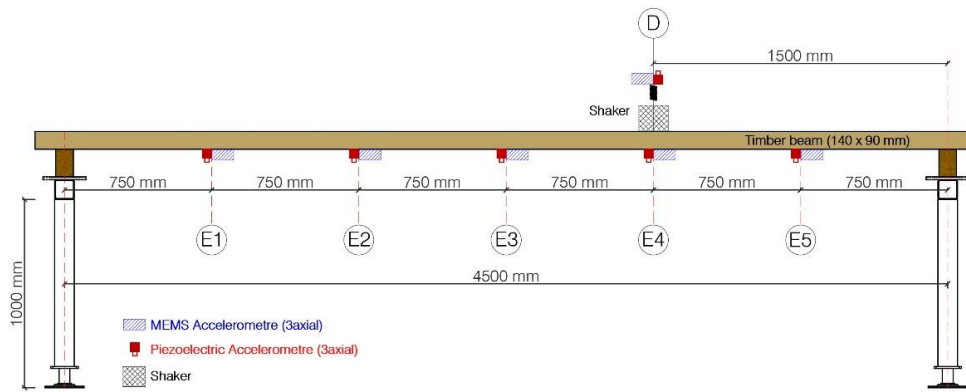


Figure 4. Measurement layout for the one-device validation test.

As can be observed in the system configuration for these first tests, which is shown in Fig. 5, the myRIO device obtained the acquire acceleration signals from the six MEMS accelerometers, and also controlled the shaker with a sinusoidal sweep signal with constant amplitude, a frequency range between 3 and 50 Hz and a duration of 3 min for the sweep. In these tests, both systems (proposed and reference) performed the acquisition simultaneously for approximately 8 min, which corresponded to almost 3 cycles of excitation.

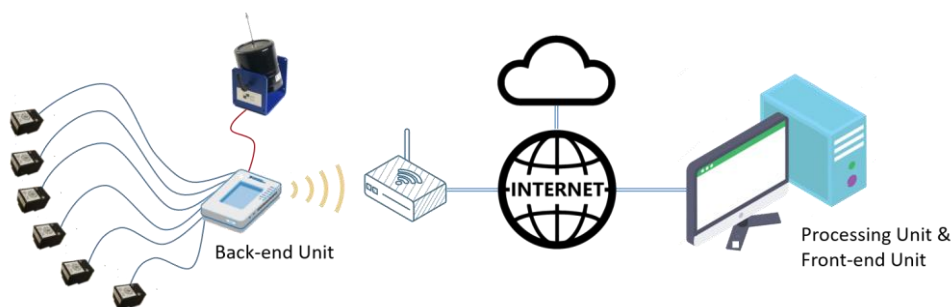


Figure 5. System configuration for the one-device validation test.

### 3.1.2. Multi-device system configuration

In order to validate a multi-device distributed system as a tool to estimate or identify the modal properties of a structure, both systems (proposed and reference) were installed on a timber platform of 1 m width, composed of 10 tightly attached timber beams (made of GLULAM 24 h) with a total length of 13.5 m, a height of 140 mm and a width of 100 mm each, as it is shown in Fig. 6. The platform is simply supported at its both ends, and two sets of three springs (each one with an elastic constant of approximately 6600 N/m) are located at the middle section, compensating the self-weight deflection. Ten pairs of accelerometers of each type (piezoelectric and MEMS) are placed on the structure drawing a  $5 \times 2$  grid, as shown in Fig. 6. In addition, to induce a controlled force on the structure, an electromechanical shaker is placed on it, as can be observed in Fig. 6, in order to excite as many modes as possible in the frequency range of interest. Due to this, two more pairs of accelerometers are required: one pair is placed on the moving mass of the shaker and another pair is located on its frame, rigidly attached to the structure and defining the driving point.

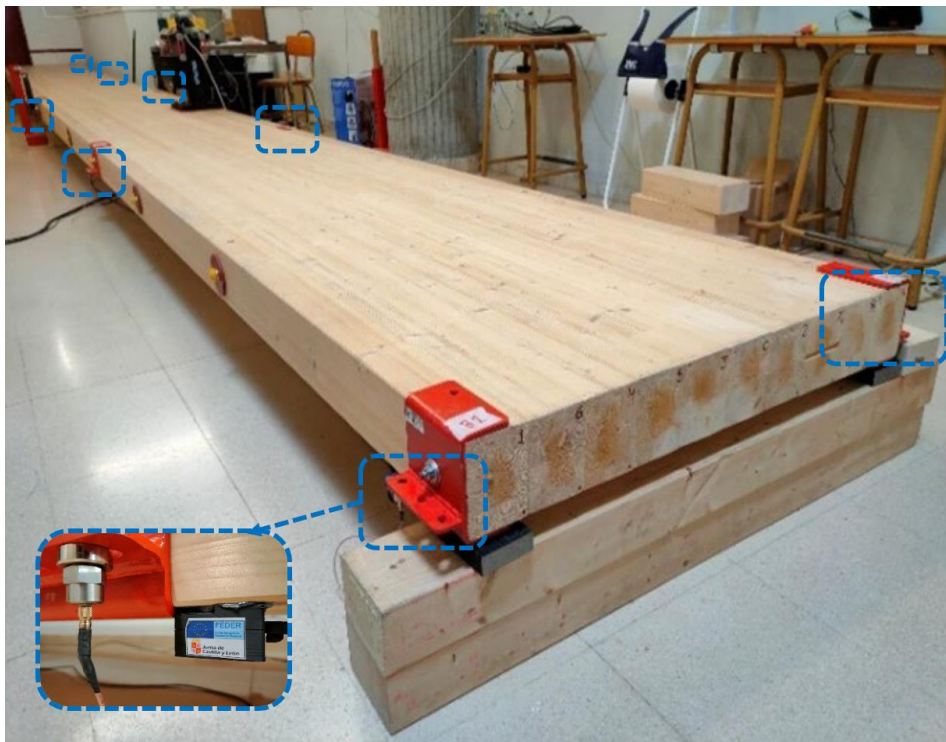
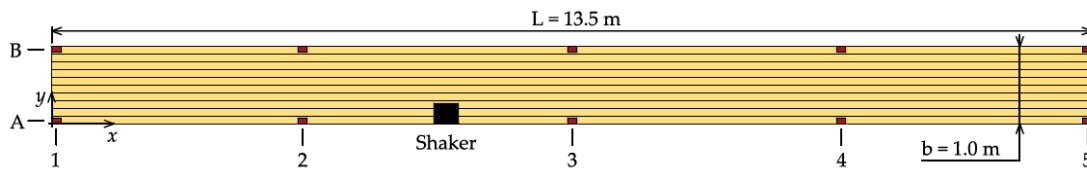
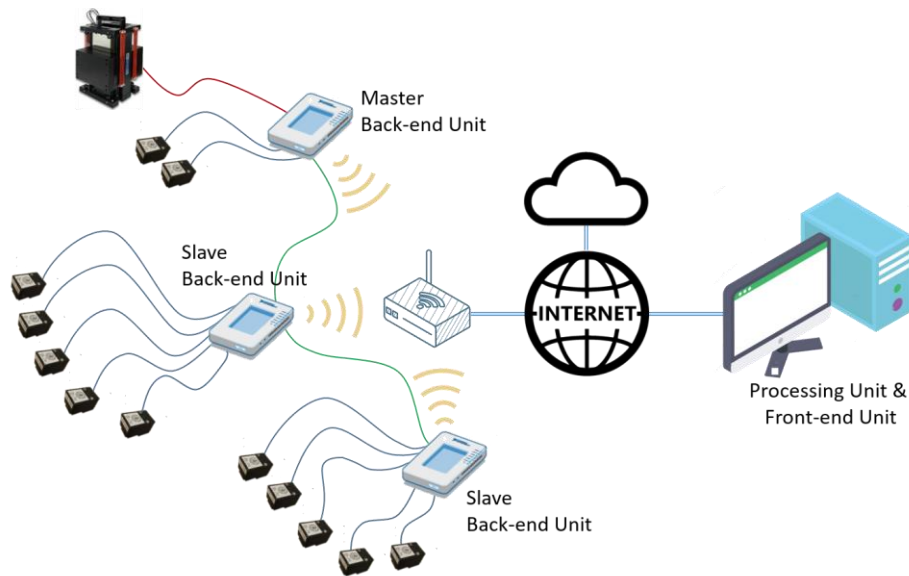


Figure 6. Measurement layout for the multi-device validation test.

As can be observed in the proposed system configuration for these second tests shown in Fig. 7, the shaker is controlled by one BE-U, generating a random noise with frequency components between 0 and 100 Hz. This BE-U, also records the signals acquired by the two MEMS accelerometers placed on the shaker, and two BE-U's more record the response of the ten MEMS accelerometers installed on the structure. All the BE-U's defined in the configuration record information at 4000 S/s during 660 s.



**Figure 7.** System configuration for the multi-device validation test.

### 3.2. Validation results

#### 3.2.1. One-device system results

The objective of the first set of tests was the validation of the accuracy of the proposed system. So, in order to achieve this objective, the response of the timber beam was analyzed in both time and frequency domains.

In order to compare the proposed system with the reference one in the time domain, the acquired signals of each system have been recorded, preprocessed with a low-pass FIR filter (1 kHz cut-off frequency, 106 coefficients, and Kaiser window with 0.005 ripple) and aligned to match the starting time. As one example, Fig. 8 shows the excitation signals registered with both systems by the accelerometers placed under the shaker (position E4 in Fig. 4). As it is usual when the response of a structure subjected to sinusoidal excitation is obtained, high amplitudes reveal the coincidence of the input frequency with the resonance frequencies of the structure, while low amplitudes correspond to frequencies to which the structure is less sensitive. The comparison of the measurements of the sensors shows a great similarity in the data provided by both systems with minor variations, that can be caused by the different location along the beam. Due to the volume that the accelerometers themselves occupy; it is impossible to place them in exactly the same geometric position, and it was decided to carry out the measurements simultaneously with both systems, to ensure that the conditions under which the tests were carried out were the same. The cross-correlation between these corresponding acquired pair of signals has been analyzed, resulting in a correlation coefficient of 0.9985.

The signals obtained by each of the six pairs of accelerometers were processed by each corresponding system to calculate the FRFs of the test structure by using a 32,768 points (8.192 s at 4000 samples/second) Blackman window, leading to a frequency resolution of 0.366 Hz. In the case of the proposed system, the FRFs were calculated using a custom LabVIEW software. Fig. 9 shows the comparison of the FRFs obtained by each system in the range of interest.

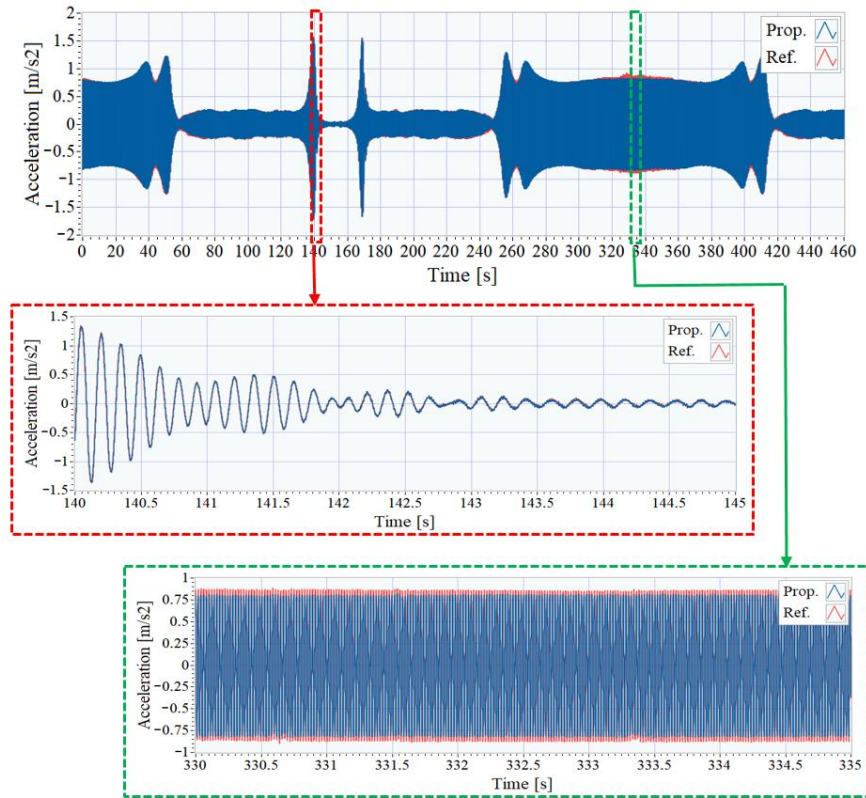


Figure 8. Time signals of accelerometers at position E4.

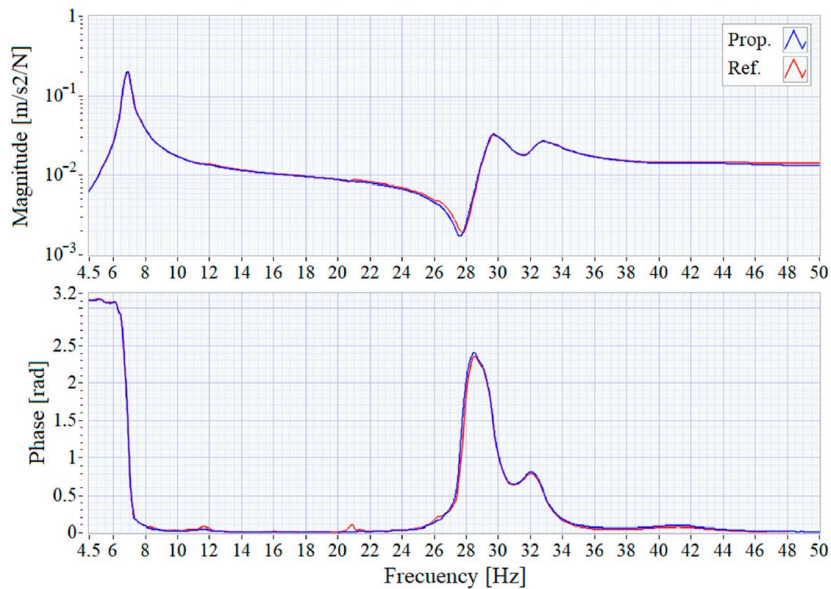


Figure 9. Frequency Response Function from 4.5 to 50 Hz.

As can be observed, the small discrepancies observed in the time domain recordings result in minimal changes in the frequency domain responses, validating of the proposed system for modal analysis of structures. In both FRFs, a main resonance peak around 6.9 Hz can be clearly distinguished. These FRF graphs show that the results obtained with the two systems are almost identical, being the cost

associated to the proposed system for this test configuration, ten times lower than the cost of the reference system, as it is detailed in Table 1. This cost difference could be even higher if the cost of the proposed system is compared to brands in the upper segment of the market or if it is considered that each accelerometer of the proposed system is triaxial, when the reference ones are uniaxial.

### 3.2.2. Multi-device system results

The objective of the second set of tests was the validation of the use of the proposed system in an experimental modal identification of a structure more complex than a timber beam. In this case, several myRIO devices needed to be employed to acquire the acceleration signals associated to the vibrating structure. So, for this new configuration, the synchronization of the proposed system if it is formed by several myRIO devices needed to be validated.

As the first step in these new validation tests, the synchronization between the BE-U's was assessed to verify that the acquisition was properly performed. Thus, three myRIO devices were used, the same number that were going to be used in the second part of these validation tests. One of them acted as Master BE-U and the other two were the Slaves BE-U's, each one connected by a 1 m long synchronization cable to the Master unit. In this previous test, a delay between the synchronization clock and the BE-U acquisition clocks of about 50 ns was measured. This delay was partly due to the propagation delay through the synchronization cable, and also included a fixed delay due to the clock regeneration algorithm. Conversely, it was observed that all the sampling clocks, reconstructed by each BE-U, were almost in phase, with a delay between them below 10 ns. Additionally, some synchronization tests using 10 m-long cables were carried out. In this case, the delay between the synchronization clocks was no greater than 55 ns. Considering that the maximum sampling period was 250  $\mu$ s, due to the sampling frequency being 4 kHz, it could be concluded that the data acquired using the distributed system was synchronous enough for the purposes intended in this new validation tests, which was the experimental modal identification of a timber platform.

Once that it was confirmed that the synchronization between the BE-U's was reliable, the experimental modal identification of the timber platform was carried out. As the first step, the FRFs of the structure were estimated separately by each system by using the recordings of the corresponding pair of 12 accelerometers, using the estimated force induced by the shaker as the input to the system and the remaining 11 accelerometers signals as the outputs of the system, leading to a total of 11 FRFs. To perform the FRFs computation, the time signals are segmented with a Hanning window of 120 s length (480,000 samples), leading to a frequency resolution of 0.0167 Hz. The computed FRFs associated to the side A of the structure (Fig. 6 above picture) are shown in Fig. 10. Subtle differences can be appreciated between both sets of FRFs, which are mainly due to slight misplacements of the sensors that compose each co-located pair (see Fig. 6, below picture). However, these differences are not significant in the surroundings of main peaks of the magnitude plots, which are representative of the structural dynamic behavior.

After estimating the FRFs, they were processed in order to estimate the properties of a set of modes: natural frequency, damping ratio and mode shape, using the Frequency Domain Parameter Identification algorithm (FDPI) [18,19]. The identified modal properties were then compared to the ones obtained after processing the FRFs issued by the reference system with a more robust and powerful method [20].

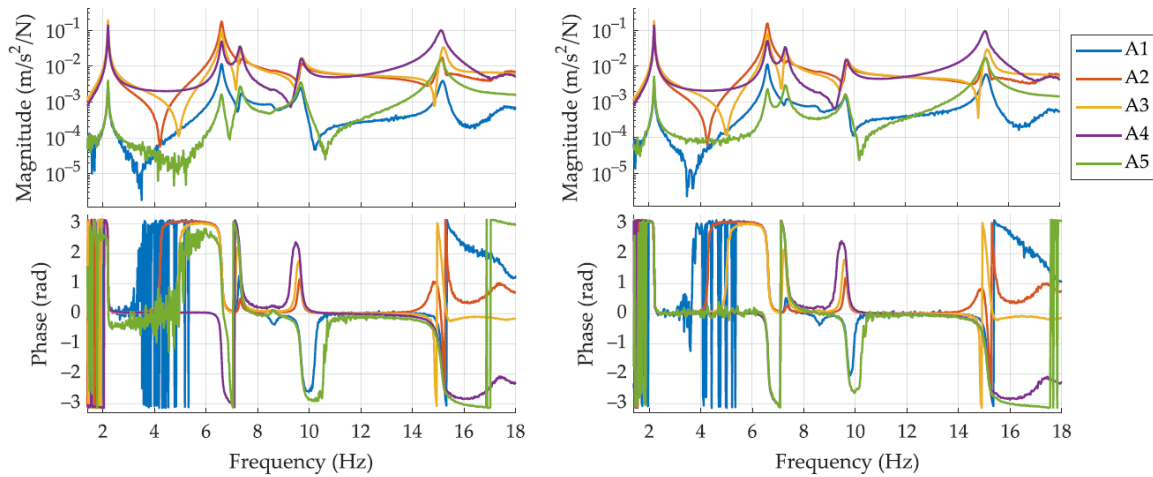


**Figure 10.** FRFs corresponding to points A1 to A5 estimated by means of the reference system (left) and the proposed system (right).

The identified natural frequencies and damping ratios are shown in Table 2. The values obtained with the proposed system and the FDPI algorithm were compared to the ones obtained with the reference system and the reference algorithm by means of the relative error, whose expression is shown in Equation (1) and where the symbol  $x$  may stand for the natural frequency or the damping ratio. As can be observed, in order to compute this relative error, the estimates provided by the reference system (RF) were taken as the trustfully ones and the properties obtained by means of the proposed system (FDPI) were compared against them. Moreover, the identified mode shapes were compared through the known as Modal Assurance Criterion (MAC) [20], and they are also shown in Table 2 and in Fig. 11.

$$\epsilon = 100 \cdot \frac{x_{FDPI} - x_{RF}}{x_{RF}} \quad (1)$$

**Table 2.** Estimated modal properties.

Mode	Natural Frequency (Hz)			Damping Ration (%)			MAC
	RF	FDPI	Error (%)	RF	FDPI	Error (%)	
1	2.198	2.190	-0.377	0.389	0.436	11.90	0.999
2	6.602	6.600	-0.049	0.709	0.744	4.91	0.997
3	7.324	7.361	0.508	0.910	1.050	15.40	0.981
4	9.685	9.669	-0.165	0.802	0.812	1.35	0.995
5	15.070	15.050	-0.135	0.931	0.779	-16.30	0.994
6	24.150	24.140	-0.037	0.684	0.674	-1.55	0.942
7	26.790	26.710	-0.032	1.100	1.080	-2.10	0.973
8	28.230	28.060	-0.599	1.080	1.200	10.60	0.953
9	39.560	39.130	-1.080	0.977	1.020	4.80	0.989

As it is shown in Table 2, there is a high correspondence between the modal properties estimated by using the proposed system and the ones estimated by using the reference one. The relative error

between both sets of natural frequencies, is under 1.1% in all cases, being the difference smaller than the frequency resolution (0.0167 Hz) in some of them. Damping ratios show higher error values, greater than 15% in a pair of cases. This may be due to this magnitude is always affected by higher uncertainty levels, and it usually evidences more variability. For this reason, the results obtained here are considered to be within the normal bounds. The MAC column shows the success in estimating the mode shapes, as this value increases towards 1 when two modes shapes are similar.

A more complete comparison by calculating the MAC value associated to the mode shapes of different mode number was carried out. These MAC values are expected to be significantly lower to 1 if the mode shapes are different enough. The complete comparison is shown in the MAC matrix in Fig. 11. In this case, the white colour corresponds to a null MAC value, whereas the solid black colour indicates a MAC value that equals 1. Intermediate values are represented with yellow, orange and red colours in ascending order. It can be observed that the main diagonal is mostly black, according to the values in the last column of Table 2, whereas the values outside the main diagonal are mostly yellow and white, evidencing, as expected, the lack of similarities between the rest of pairs of mode shapes.

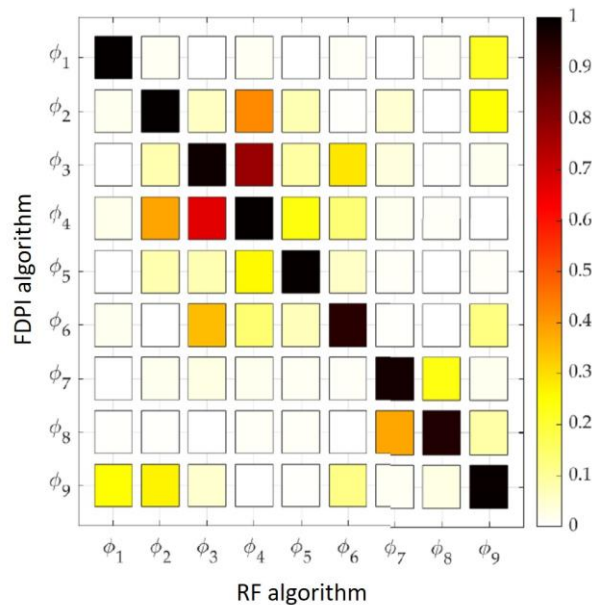


Figure 11. MAC matrix of the mode shapes estimated through the RF and the FDPI algorithms.

#### 4. CONCLUSIONS

This paper presents a low-cost system for monitoring the structural health (SHM) based on MEMS sensors. The architecture consists of back-end units devoted to recording the signals collected by the MEMS accelerometers, as well as generating the excitation signals. The processing units are in charge of pre-processing the signals in the time domain, calculating the FRFs and, finally, performing the modal analysis of the structure. The whole process is controlled by the front-end units.

The proposed architecture based on these modules provides a scalable, reconfigurable and low-cost system compared to commercial systems based on analog sensors and acquisition systems with high-performance analog-digital converters. Validation tests has been carried out, based on one or several units based on a myRIO platform together with some digital MEMS accelerometers, placed on different

timber structures, and connected in order to synchronously acquire data from all sensors. The obtained results have validated that the proposed low-cost system is able to synchronously measure data useful to accurately perform the complete modal analysis of a structure.

## ACKNOWLEDGEMENTS

This research was funded by the Junta de Castilla y León, co-financed by the European Union through the European Regional Development Fund (ref. VA095P17 and VA228P20). Additionally, the partial support through the RTI2018-098425 project, Spanish Government, is acknowledged.

## REFERENCES

- [1] Ye, X.W.; Jin, T.; Yun, C.B. (2019). A review on deep learning-based structural health monitoring of civil infrastructures. *Smart Structures and Systems*, 24, 567-585.
- [2] Farrar, C.R.; Doebling, S.W.; Nix, D.A. (2001). Vibration-based structural damage identification. *Philosophical Transactions of the Royal Society A: Mathematical, Physical and Engineering Sciences*, 359, 131-149.
- [3] Mahammad, A.H.; Kamrul, H.; Ker, P.J. (2018). A review on sensors and systems in structural health monitoring: Current issues and challenges. *Smart Structures and Systems*, 2, 509-525.
- [4] Farrar, C.; Worden, K. (2006). An introduction to structural health monitoring. *Philosophical Transactions of the Royal Society A: Mathematical, Physical and Engineering Sciences*, 365, 303-315.
- [5] Matos, J.C.E. et al. (2009). Health Monitoring System (HMS) for structural assessment. *Smart Structures and Systems*, 5, 223-240.
- [6] Soria, J.M. et al. (2016). Vibration monitoring of a steel-plated stress-ribbon footbridge: Uncertainties in the modal estimation. *Journal of Bridge Engineering*, 21, C5015002.
- [7] Girolami, A.; Brunelli, D.; Benini, L. Low-cost and distributed health monitoring system for critical buildings. In 2017 IEEE Workshop on Environmental, Energy, and Structural Monitoring Systems (pp. 1-6). New York: Institute of Electrical and Electronics Engineers (IEEE).
- [8] Salawu, O. (1997). Detection of structural damage through changes in frequency: A review. *Engineering Structures*, 19, 718-723.
- [9] Ribeiro, R.R.; Lameiras, R.D.M. (2019). Evaluation of low-cost MEMS accelerometers for SHM: Frequency and damping identification of civil structures. *Latin American Journal of Solids and Structures*, 16.
- [10] Acar, C.; Shkel, A.M. (2003). Experimental evaluation and comparative analysis of commercial variable-capacitance MEMS accelerometers. *Journal of Micromechanics and Microengineering*, 13, 634-645.
- [11] Zhu, L. et al. (2018) Development of a High-Sensitivity Wireless Accelerometer for Structural Health Monitoring. *Sensors*, 18, 262.

- [12] Tan, T.D.; Anh, N.T.; Anh, G.Q. Low-cost Structural Health Monitoring scheme using MEMS-based accelerometers. In 2011 Second International Conference on Intelligent Systems, Modelling and Simulation (pp. 217–220).
- [13] Rosal, J.E.C.; Caya, M.V.C. Development of Triaxial MEMS Digital Accelerometer on Structural Health Monitoring System for Midrise Structures. In 2018 IEEE 10th International Conference on Humanoid, Nanotechnology, Information Technology, Communication and Control, Environment and Management (pp. 1–5).
- [14] DS-SIRIUS Data-Logger. <https://dewesoft.com/products/daq-systems/sirius>
- [15] ADXL355 3-Axis MEMS Accelerometer. [https://www.analog.com/media/en/technical-documentation/datasheets/adxl354\\_355.pdf](https://www.analog.com/media/en/technical-documentation/datasheets/adxl354_355.pdf)
- [16] myRIO Platform. <https://www.ni.com/pdf/manuals/376047c.pdf>
- [17] KS76C.100 IEPE Accelerometers. [https://mmf.de/standard\\_accelerometers.htm](https://mmf.de/standard_accelerometers.htm)
- [18] Böswald, M. et al. A review of experimental modal analysis methods with respect to their applicability to test data of large aircraft structures. In 2006 International Conference on Noise and Vibration Engineering (pp. 2461-2482).
- [19] Lembregts, F.; Leuridan, J.; Van Brussel, H. (1990) Frequency domain direct parameter identification for modal analysis: State space formulation. *Mechanical Systems and Signal Processing*, 4, 65-75.
- [20] Maia, N.; Silva, J. (1997). Theoretical and Experimental Modal Analysis; Engineering Dynamics Series; Research Studies Press: Baldock, UK.